Journal of Power Sources 222 (2013) 267–276

Contents lists available at SciVerse ScienceDirect

Journal of Power Sources

journal homepage: www.elsevier.com/locate/jpowsour

Control of a solid oxide fuel cell system with sensitivity to carbon formation☆

Matthew J. Kupilik*, Tyrone L. Vincent

Department of Electrical Engineering and Computer Science, Golden, CO 80401, USA

HIGHLIGHTS

- ► Develops a nonlinear, first principles model of a SOFC system, including all balance of plant components.
- ► Reformate composition is modeled and experimentally verified, allows for control of reformer.
- ► Equilibrium chemistry is applied to calculate reformate quality with respect to solid carbon formation.
- ► Novel implementation of a linear parameter varying model reduction.
- ► Includes application of model predictive control to a linear parameter varying model.

ARTICLE INFO

Article history:
Received 3 July 2012
Received in revised form
27 August 2012
Accepted 29 August 2012
Available online 7 September 2012

Keywords:
System identification
Model predictive control
SOFC systems
Linear parameter varying
Renewable energy systems

ABSTRACT

Fuel cells allow for increased efficiency in power production when compared to the thermodynamically limited efficiencies of heat engines. In the case of solid oxide fuel cells, they are also usable with the fuel infrastructure currently in place (natural gas). Although potentially transformative, solid oxide fuel cells are currently limited by engineering challenges related to operating temperature (>600 °C), durability, and load following ability. For example, the buildup of solid carbon in the stack, or coking, potentially limits one of the most desirable aspects of solid oxide fuel cells, which is their robustness to fuel type. As the working temperatures for SOFCs continue to decrease, in order to maintain fuel robustness, the need for control of the inlet fuel composition increases. This work demonstrates the use of a model predictive control algorithm on a solid oxide fuel cell system including reformer, blowers, heat exchanger, tail gas burner and stack. The controller allows for load following demand changes from the fuel cell and meets those demand changes, while ensuring that the reformate composition is not prone to solid carbon formation. The controller meets current demand changes to within 0.1 A s^{-1} while maintaining compositional limits on the reformate flow and temperature limits on the stack and reformer.

1. Introduction

The use of solid oxide fuel cell (SOFC) systems in both portable and fixed installation continues to be the subject of significant research. The high temperatures required for electrolyte conductivity remain an engineering challenge. Current systems employing yttria stabilized zirconia electrolytes tend to operate at approximately 700–800 °C. At these high temperatures internal reforming of hydrocarbon based fuels is possible [1]. However, solid carbon formation, or coking, is still a threat to system durability and robustness. Much current work is focused on lowering the operating temperatures of SOFC systems. Lower temperatures result in a more efficient electrochemical process and significantly lessen the costs of external components such as blowers, heat sinks, and transport systems. Currently proposed SOFC electrolyte types allow for operation at temperatures as low as approximately 400 °C [2]. At these temperatures external fuel reforming becomes even more important to avoid coking in the stack, as the level of internal reforming is reduced [2]. The need for external reforming is even greater when biogas is the fuel source [3]. The goal of this research is to examine if a control algorithm can be designed to control the flow rates of fuel and air to the stack such that the demand current is produced, coking does not occur and the operational limits of the fuel reformer are maintained. The system to be controlled is a potentially mobile 1.5 kW SOFC system. Catalytic partial oxidation (CPOX) reforming has been chosen as it allows faster response times, and the addition of steam is not required. The use of steam or auto-thermal reforming, although more efficient, decreases response time and can be problematic for mobile systems. Air is

☆ This work was supported by the Department of Energy, Office of Energy Efficiency and Renewable Energy, Grant DE-FG36-08G088100.

* Corresponding author. Tel.: +1 303 908 1624; fax: +1 303 273 3602.
E-mail addresses: mkupilik@mines.edu, redpointed@yahoo.com (M.J. Kupilik), tvincent@mines.edu (T.L. Vincent).

0378-7753/$ – see front matter © 2012 Elsevier B.V. All rights reserved.
http://dx.doi.org/10.1016/j.jpowsour.2012.08.083

assumed to be available and both fuel and air are moved through the system using blowers.

Control of SOFC systems is challenging due to non-linear system dynamics and the existence of multiple temperature and compositional operating constraints. System components have temperature based operating limits, and the stack has fuel inlet composition and utilization constraints, including avoiding solid carbon formation. Model predictive control (MPC) is a proven control method for meeting constraints, but requires a model that can be optimized in real time. Nonlinear models that capture these constraints are too complex to optimize in real time within a model predictive controller. The approach taken in this work is to create a first principles model that captures the operating constraints, perform a system reduction to obtain a set of linear parameter varying (LPV) models, and implement model predictive control on the resulting LPV model.

The constraints captured include temperatures of inlet and outlet flows from all components, spatially varying temperature of the cell tubes within the stack and heat exchanger and a measure of whether the fuel supplied from the reformer to the stack is prone to solid carbon formation. These constraints provide the motivation for a set of identification operations carried out using the first principles model. This simulation produces input–output data which is then used to identify the LPV model. In effect, the high order non-linear model is used as a simulated experiment to identify the LPV model. The LPV model is actually a set of linear models which are combined or blended using a function of a measured signal. A linear model is calculated at each time step for which the scheduling variable is measured. This linear model is then used to solve the MPC optimization problem to find the new inputs for the system when the controller is implemented.

The proposed method could easily be implemented for any fuel reformer type or stack geometry for which an accurate first principles model exists. Hybrid identification schemes are also possible, where a specific fuel reformer geometry or blower is modeled and used to produce input/output data. The reformer model outputs can then be experimentally simulated and applied to a physical system. The resulting input/output combination can then be used to identify a system wide model for use in model based control. Thermal effects between modeled and experimental components will not be captured for such a hybrid identification scheme.

2. Fuel cell system

The first challenge in developing a model to be used for model based control is determining the level of fidelity. Extremely high order computational fluid dynamics (CFD) models can be created to match very specific geometries and such models capture both the spatial and time varying aspects of the system. Such models are tailored very specifically to the geometries involved and impose a prohibitive computational burden. As such they are most suited as analysis and design tools rather than for control. SOFC systems can also be modeled using lumped thermodynamic models, enforcing mass and energy conservation, but ignoring spatial dynamics and chemical kinetics. Such models also ignore the kinematics at the reformer catalyst and the cells. These effects are important to the operation of the SOFC system and cannot be ignored. Hot spots can occur spatially along cell tubes [4], and the reformate composition is highly dependent on the reaction kinetics at the catalyst [5]. Both these factors impose operating constraints on the system. The model utilized within the controller has to suitably capture such dynamics while still being fast enough that solving an optimal control problem in real time is feasible.

In order to capture the dynamics of the system as closely as possible, we initially develop a non-linear first principles model of the system. This non-linear system model consists of the following (all components are sized for a kilowatt order system):

- Blowers: one to provide air to the fuel reformer, and one to provide air to the stack.
- Fuel reformer: a catalytic partial oxidation reactor which produces the hydrogen rich gas used as a fuel for the stack.
- Fuel cell stack: a collection of tubular solid oxide fuel cells which produces the desired current.
- Tail gas burner: simple burner to combust any remaining fuel products in the stack exhaust in order to help pre-heat air.
- Heat exchanger: a counter-flow tubular heat exchanger to capture heat from the stack exhaust and preheat the stack inlet air.

The blowers are modeled via first principles as in [6]. The blower model is based off a commercially available blower, an EBM D1G133-DC13-52, which has been rescaled using the fan laws [7]. The result allows for the calculation of the mass flow as a function of the motor speed and the required pressure differential. Manufacturer data is used to fit a function for the motor speed and the power provided to the blower. No blower is used for the fuel flow to the reformer as it assumed to be under sufficient pressure.

The fuel reformer is considered as a continually stirred tank reactor with surface chemistry. A CSTR was used as it is the lowest dimensional model that can capture the temperature and composition of the reformate. Although a plug flow model would be more accurate, only the final exit composition and temperature are used. The reformer has a tubular geometry with a rhodium catalyst on a foam monolith. The model makes use of the reaction mechanism for natural gas over rhodium developed in [5]. The model itself has been validated against an experimental CPOX reactor at the Colorado Fuel Cell Center [8]. Reformate composition and temperature are considered as functions of the input fuel compositions, temperatures and the mass flow rate and temperature of the air provided to the reformer. For the purposes of identification and control the input fuel is biogas with a composition of 70% CH_4 and 30% CO_2. Biogas was used as an input fuel to test the system with a high carbon content fuel, challenging from a coking standpoint. The biogas content was chosen as 70% CH_4 and 30% CO_2 since this composition is within the range of that produced by sewage plants and agriculture. The model, however, fully supports temporal variations in inlet fuel composition and temperature.

The stack model is a combination of high order spatially discretized single tubular cell models. Compositional and temperature variations are captured along each tube length. The model captures heat transfer inside each cell, and from a cell to the gas outside. Thermal effects from cell to cell are not included. To model a stack, 100 tubular cells are connected electrically in series and in parallel with respect to mass flows. The sizes of the tubes are taken as 15 cm long with an outer diameter of 1 cm. The tubular cell model is described in detail in [9].

The tail gas burner is simulated using an axisymmetric flame model in Cantera [10]. The heat exchanger is modeled using a dynamic counter-flow tubular heat exchanger model which allows for varying temperature and composition in the inlet flows. A detailed description of the heat exchanger model is available in [11]. The physical parameters of the SOFC system are shown in Table 1. Together the system model allows for solutions of the gas flow compositions and temperatures throughout the system. A diagram of the SOFC system and its connections is shown in Fig. 1.

Analysis of the system model provides excellent motivation for the development of an MPC controller to ensure stable and safe operation of the system. For example, with both the fuel reformer and stack air flows supplied via blowers, the dynamic response of the blowers is critical to the ability of the reformer and stack to

Table 1
SOFC system physical parameters.

Parameter	Value
Fuel reformer	
Inner diameter	0.0082 m
Length	0.0165 m
SOFC stack	
Cell outer diameter	0.1 m
Cell length	0.15 m
Heat exchanger	
Wall material	2205 stainless steel
HX length	0.25 m
Inner tube diameter	0.025 m
Outer tube diameter	0.040 m
Wall thickness	0.005 m
Blowers	
Efficiency	0.38
Rotational inertia	4×10^{-8} kg m^2

respond to demand changes. For large increases in current demand, the supply of fuel to the reformer can be increased much more quickly than the air, which will result in compositions that temporarily have very low ratios of O_2/CH_4, and this can lead to carbon deposition in the stack. An increased current load can also produce very undesirable fuel utilization because the air blower time constant is slower than that of the reformer fuel supply. This effect is shown in Fig. 2 for step changes in between different operating conditions. The simulation in Fig. 2 involves step changes across a variety of operating conditions, from low current (approximately 5 A) with fuel utilization varying from 45% to 76% and O_2/CH_4 ratios from 1.13 to 1.52. The "spikes" present in the current and exhaust H_2% in Fig. 2 are due to air flow delay induced by the blowers. Large changes in current require large changes in mass flow of both fuel and air. The fuel delivery system is much faster than the blowers delivering air. Thus air/fuel ratios can become very skewed, resulting in undesireable transients in both current and H_2 exhaust. The magnitude of these transients is dependent on the dynamics of the blower model, but the simulation shows that to avoid these transients, the controller must account for any mismatch in dynamics between air and fuel delivery subsystems. An implemented controller must be able to choose between the various mass flow, O_2/CH_4 ratio combinations in order to produce the desired current without violating temperature, utilization, and coking constraints.

3. System constraints

There are several operating regions that need to be avoided for the SOFC system. These operating regions are dependent on both the composition of the gases and the temperatures of the components themselves. It is well documented that model predictive control can respond to current disturbances and maintain the required stack temperatures [12]. However, compositional constraints have a larger impact on the available operating regions. These include ensuring the fuel utilization, as measured by the H_2 percentage in the stack exhaust, does not decrease below a minimum percentage and that the reformate composition is not prone to forming solid carbon. These operating constraints are summarized in Table 2.

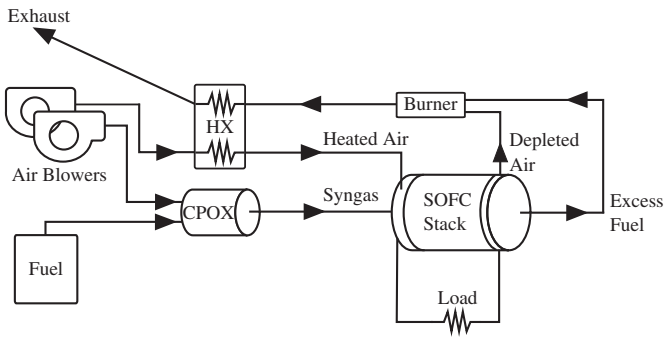

Fig. 1. SOFC system block diagram.

3.1. Temperature constraints

The CPOX fuel reformer consists of a catalyst on a foam monolith which encourages an exothermic reaction in order to produce a suitable fuel for the stack. Since this reaction is exothermic, temperatures can easily exceed the sintering temperature of the catalyst. Operating the reformer at too low a temperature, however, can cause coking, which leads to catalyst deactivation. Thus ensuring the temperature of the reformer is within prescribed limits forms one of the output constraints for the system controller. The temperature limits for the reformer were set to what was experimentally considered "safe" for a lab based CPOX reformer at the Colorado Fuel Cell Center. The upper limit is to avoid sintering and the lower limit is the temperature the reformer was pre-heated to before fed fuel, in order to alleviate coking. In addition to the temperature constraints on the reformer, the temperature of the stack itself needs to be regulated within a prescribed limit. If too low a temperature is set, the electrolyte is no longer conductive; if the stack temperature is too high, seals and other components can be damaged. The temperature limits for the stack were set to bracket the expected operating conditions. A lower limit is not set, as the controller ensures that the temperature is sufficient to produce the demand current. The upper limit is set to an estimated minimum temperature to produce the operating range of current (5–25 A).

3.2. Hydrogen utilization

Fuel utilization is an important variable in SOFC system control. Very low fuel utilizations (and thus very high exhaust concentrations of H_2) are to be avoided as inefficient and wasteful. Very high fuel utilizations (very low exhaust H_2 concentrations) indicate fuel depletion and can cause cell damage as well as inability to meet current demand. The fuel utilization is calculated as:

$$1 - \frac{\dot{m}_{\text{out}} H_{\text{comb,out}}}{\dot{m}_{\text{in}} H_{\text{comb,in}}}.$$

Where $\dot{m}_{\text{out}}$ is the mass flow of depleted fuel, $\dot{m}_{\text{in}}$ is the mass flow of fuel into the stack (both in kg/sec), and $H_{\text{comb},x}$ is the heat of combustion of whatever composition is being used. How this utilization exactly relates to the H_2% in the stack exhaust is a function of the composition of the reformate, the mass flows, and the operating temperature. Generally, however, if the utilization is very high, then the H_2 in the stack will be low. The primary control variable of interest is the H_2% in the exhaust. The minimum value of 2.5% is arbitrarily chosen to prevent re-oxidation of the anode. The actual exhaust H_2% is allowed to vary in order to meet transient current demands as quickly as possible without violating this minimum. The maximum H_2% exhaust concentration is not limited but the controller is designed to have a preferred operating value of 5%. This exhaust concentration corresponds to a fuel utilization of 70–75%.

3.3. Reformate carbon deposition

The deposition of solid carbon is analyzed using thermodynamic equilibrium chemistry amongst the important species. The method

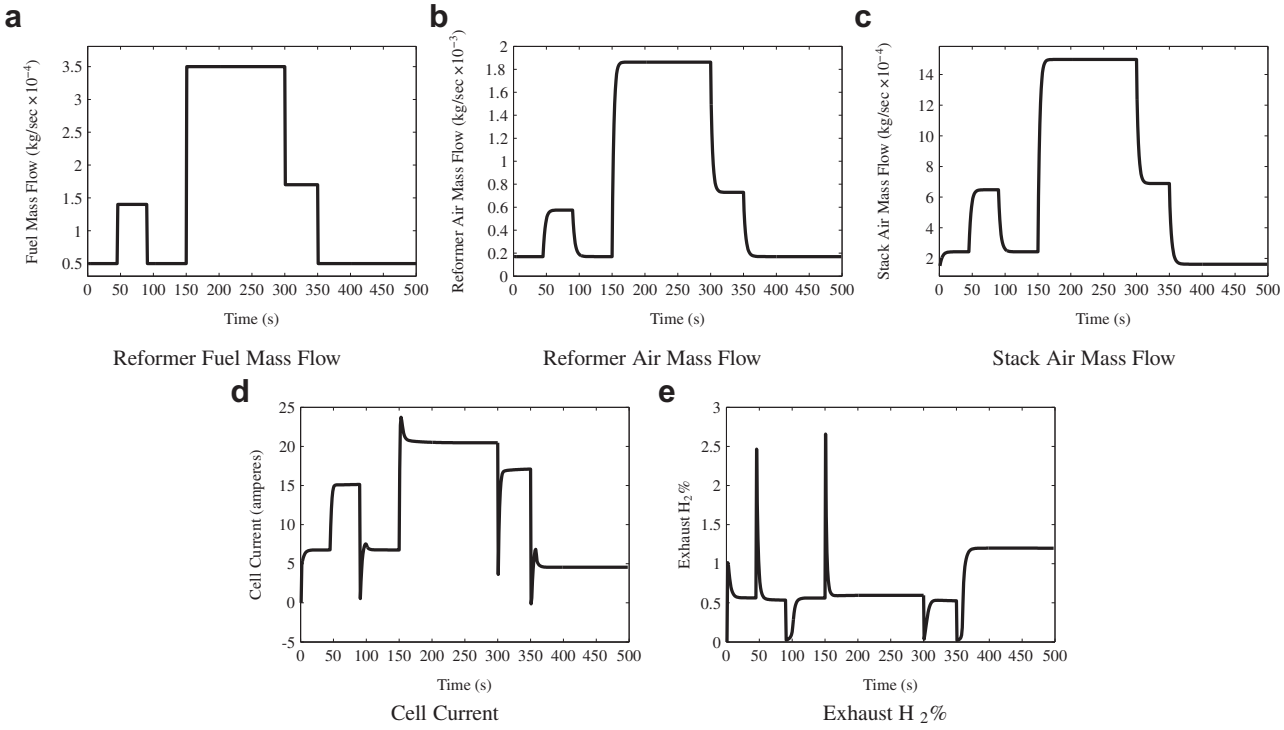

Fig. 2. Open loop dynamic response.

used is that developed by [13], which was expanded to create reforming fuel maps in [14]. The determination of whether a fuel can produce solid carbon is found using the temperature and partial pressures of H_2, CH_4, CO, CO_2, and H_2O. Other species are considered inert and the partial pressures of the active species are normalized with respect to the inert species. Considering the following reactions:

$$\begin{aligned} CH_4 &\leftrightarrow C + 2H_2 \\ H_2 + 2CO &\leftrightarrow C + H_20 \\ 2CO &\leftrightarrow C + CO_2, \end{aligned} \tag{1}$$

we calculate the conditions where the net amount of C created and consumed is zero. Graphically, this can be illustrated using a ternary diagram consisting of three components, C, H, and O, as shown in Fig. 3 (all thermodynamic calculations carried out using [10]). The line where the net carbon created is zero is known as the carbon deposition barrier (CDB). It represents for a given temperature the composition of the reformate that is capable of forming solid carbon. If the reformate composition, plotted on the same ternary diagram, is below this line then solid carbon formation is unlikely. If the reformate composition is above the carbon deposition barrier (CDB) then the reformate is prone to solid carbon formation. The distance measure used is orthogonal to the H–O axis of the ternary diagram. This measure was used as the actual value of interest is whether the reformate composition lies above or below the CDB curve. This analysis is based solely off equilibrium chemistry and does not consider the material properties of the cell. The provided measure of carbon formation is not intended to replace a detailed kinematic analysis. However, since the object is to control the reformate composition it provides a measure of "reformate quality" as far as carbon deposition, which has mostly been ignored in previous SOFC system control methods.

Table 2
SOFC system constraints.

Parameter	Value
MEA temperature	$T_{fc} < 1200$ K
Reformer temperature	650 K $< T_{cx} <$ 1075 K
Exhaust H_2%	≥2.5%
CDB distance	≥0.0

4. System model reduction

Model reduction via system identification is a technique to identify a dynamic model using experimental data. For the previously described SOFC model, the system is described by a large number of non-linear differential and algebraic differential equations. Model

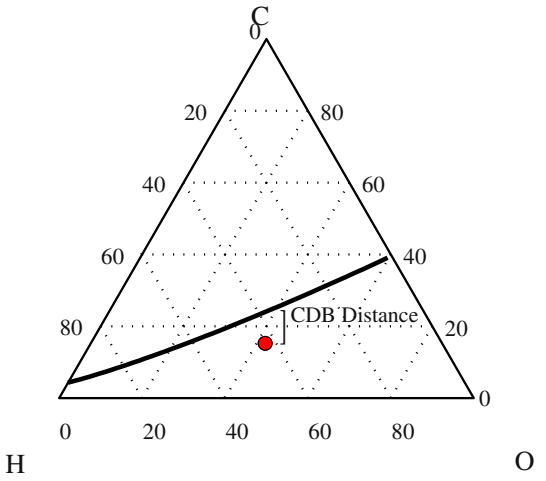

Fig. 3. Fuel ternary diagram, CDB for 894.76 K (black), reformate composition with inlet $O_2/CH_4 = 1.97$ (red). (For interpretation of the references to colour in this figure legend, the reader is referred to the web version of this article.)

evaluations can take on the order of a minute for large changes in system state. Although this model is easily accurate enough for control purposes, the non-linearity and evaluation time make it unsuitable for use in a model predictive controller. Ideally a single linear model could be found that would allow for a fast optimal control of the system, however, due to the large non-linearities present over the operating range, no such model exists. Thus the use of a combination of linear models which are blended using a function of measured signals (LPV) is chosen to represent the SOFC system.

Several approaches in the field of system identification work to solve this problem. Subspace LPV identification was chosen as it creates a state space model, suitable for model predictive control. Subspace LPV identification algorithms can be divided into two approaches, local and global. Local approaches find linear models around operating points and interpolate between them using a function of a measured quantity. Global approaches attempt to excite all desired non-linearities in the system in a single experiment, and then fit the model based on a functional dependence to one or more measured quantities.

We use a LPV global approach to the identification problem, described in detail in [15] and implemented in [16]. The model structure is given in Eq. (2),

$$\begin{aligned} x_{k+1} &= \sum_{i=1}^{m} \mu_k^{(i)} \left(A^{(i)} x_k + B^{(i)} u_k + K^{(i)} e_k\right) \\ y_k &= C x_k + D u_k + e_k. \end{aligned} \tag{2}$$

Where $x_k \in \mathbb{R}^n$ is the state at time k and system matrices are $A^{(i)} \in \mathbb{R}^{n\times n}$, $B^{(i)} \in \mathbb{R}^{n\times r}$, $K^{(i)} \in \mathbb{R}^{n\times l}$, $C \in \mathbb{R}^{l\times n}$, and $D \in \mathbb{R}^{l\times r}$ for a system with state size n, r inputs, and l outputs. $\mu_k \in \mathbb{R}^{m\times L}$ is a vector of scheduling variables which determines how the m different linear models are combined at each of the L time steps. $\mu_k^{(i)}$ is the ith element of μ_k. $e_k \in \mathbb{R}^l$ denotes the zero mean white measurement residual. For the SOFC system analyzed, model inputs are chosen as the variables that can be actuated. These include power to the reformer blower (p_{blo}), power to the stack blower (p_{stack}), fuel mass flow to the reformer (m_{fuel}), and the stack voltage (V). Outputs are the variables that require regulation or impose constraints. These are taken as the current (I), the membrane electrode assembly (MEA) assembly temperature (T_{MEA}), the hydrogen exhaust concentration ($H_{2,\text{ex}}$) and the temperature of the gas exiting the fuel reformer (T_{ref}) and the distance from the CDB (d_{CDB}). The input and output vectors are then defined as:

$$\begin{aligned} u_k &= \left[p_{\text{blo}}, m_{\text{fuel}}, p_{\text{stack}}, V\right]' \\ y_k &= \left[T_{\text{MEA}}, I, H_{2,\text{ex}}, T_{\text{ref}}, d_{\text{CDB}}\right]'. \end{aligned} \tag{3}$$

The algorithm reconstructs the state sequence using the known input and output data as well as the scheduling sequence. Once this is done the unknown system matrices ($A^{(i)}$, $B^{(i)}$, $K^{(i)}$, C, D, for $i = \{1...m\}$) are found via least squares. The algorithm depends on the existence of a set of measurable scheduling parameters ($\mu^{(i)}$), which linearly weight the system matrices at each time step. The choice of scheduling parameter has a strong impact on the accuracy of the identified model. Ideally, physical intuition could be used to separate the system into scheduled modes using a measured variable, however in the case of an SOFC system there are too many operating non-linearities to make this choice obvious. The stack current has been used in previous stack identification and control applications [17]. However, current does not provide a perfect scheduling parameter. There are a multitude of operating points with large variations in reformate composition, mass flow, and voltage, that all produce the same current. It is part of the control challenge to choose amongst these operating conditions. As such, utilizing only current as a scheduling variable is limiting, however, additional measurements are often available. The temperature of the stack MEA assembly can be used as a measurement, as well as the temperature of the reformate gas leaving the fuel reformer. These additional measurements can provide additional components for the scheduling sequence. Indeed, previous work has shown that the inlet composition of the fuel to the reformer can be estimated using only the reformate temperature as a measurement [8]. The results presented in this work utilize current and MEA temperature as scheduling variables.

For the identification procedure, variables to be chosen include the scheduling parameters, the number of linear models to blend, (m), the forward time window (p), and the state dimension of the resulting models, (n). Values selected are $m = 3$, $p = 2$, and $n = 7$. The model is simulated with a time step of 1 s. The range of operating conditions over which the identification data is produced must match the desired operating regions of the system. The identification data set was chosen to cover as wide a range as possible; approximately 0–25 A/cell, with both large mass flow and low mass flow conditions represented, as well as jumps between them. Identification and validation simulations are plotted within a reduced parameter space in Fig. 4. This plot represents the parameter space using three parameters which are combinations of the selected inputs and the output that we desire to regulate. The composition of fuel and air to the reformer is shown using the O_2/CH_4 ratio. The total mass flow of fuel and air to both the stack and the blower and the current are also shown. Using this parameter space it can be seen that the identification simulation is representative of the expected operating conditions. The identified data points are clustered around the steady state operating conditions represented by the red boxes. If the desired operating condition is not close to any of the identified points, we would expect the LPV model to be a poor fit. This reduced parameter space does not take into account voltage or indicate which operating conditions would violate system constraints. It does, however, allow for a visualization of the identification simulation relative to the desired operating conditions.

At each operating condition, pseudo-random binary signal (PRBS) perturbations are added; example inputs used are shown in Fig. 5. Changes from operating region to operating region were also simulated, ensuring identification of the low exhaust H_2% and carbon forming regions that the controller needs to avoid during

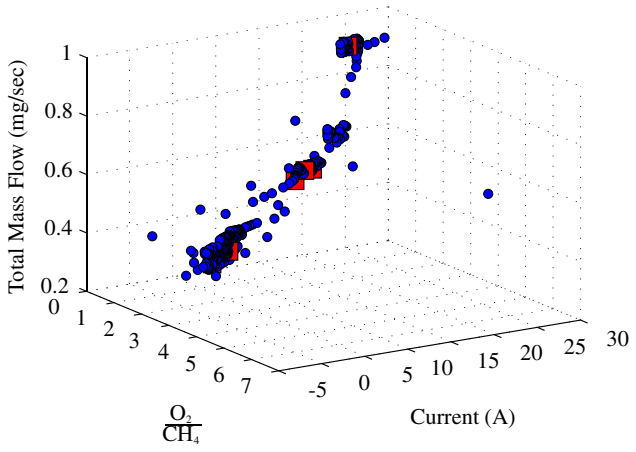

Fig. 4. Identification and validation parameter space, the validation data set is shown using red squares. The identification data set is shown using blue circles. (For interpretation of the references to colour in this figure legend, the reader is referred to the web version of this article.)

actual operation. The scheduling parameters (current and MEA temperature) are normalized to be between negative and positive one, and passed through a low pass filter with a normalized cut off frequency of 0.4. The combination of these measurable quantities allows for scheduling of an LPV model over the operating range. Identification results for a seven state, five output, four input LPV model are shown in Fig. 6. The results in Fig. 6 are given for a validation data set, using a one step ahead predictor. That is, the state is assumed to be fully measured at each time step, and the identified model is used to predict the impact of the applied inputs to the state and the outputs at the next time step. These plots thus express the accuracy of the LPV model when used in a system where all outputs are measurable and the system is fully observable. However, for the SOFC system we are interested in controlling, only three of the outputs are measurable. A more useful representation of the accuracy of the LPV model is to combine the simulation with a Kalman filter, which makes use of the model and measurements to estimate the unknown outputs. The LPV model simulated with a Kalman filter is shown in Fig. 7. Only the two estimated outputs are plotted, as the measurements are highly trusted and the model is used only to calculate the unknown outputs.

The performance of the estimated model is measured using a variance accounted for (VAF) value, calculated as:

$$\mathrm{VAF}_{y_k} = \max\left\{1 - \frac{var\left(y_k - \widehat{y}_k\right)}{var(y_k)}, 0\right\}(100). \tag{4}$$

For the desired, 4 input, 5 output system, identification of a system with three blended linear models of state size 7 resulted in the highest VAF fit for a validation data set. Using the current and MEA temperature as scheduling variables gives VAF scores (for the one step ahead predictor) of 97.8927 for the MEA temperature, 99.5377 for the current, and 99.9619 for the reformer temperature. The remaining outputs have VAF scores of 84.2987 for the exhaust H_2% and 93.8894 for the CDB distance. These values are for the same test run used in the identification simulation. When testing the identified model on data sets other than that used for identification (but still within the same operating range) the VAF scores dropped for the two unscheduled variables to approximately 80–90 for the exhaust H_2% and 60 to 90 for the CDB distance. Both temperatures are identified very well, with the LPV model predicting the nonlinear model within 0.5 K. The current also shows excellent identification with errors remaining within 1 A. The range of operation for the identification simulation is also quite challenging, consisting of a large number of operating points for the SOFC system.

4.1. Model predictive control

Model predictive control has been applied to SOFC systems previously [12,18,19] but not with a model of sufficient fidelity to estimate fuel composition throughout. The use of an LPV model allows for linear MPC to be applied where previous work has resorted to nonlinear MPC implementations. With the development of a sufficiently detailed system level model, carbon formation can be avoided and temperature limits maintained while still allowing load following. The controller signal flow diagram is shown in Fig. 8. The measurable outputs are taken from the SOFC system at each time step. The scheduling sequence is calculated from the measured outputs and used to calculate the current linear model using the LPV framework. This linear model is then used within a standard Kalman filter (along with the measurements) to obtain a full state estimate. This gives an estimate for the two unmeasurable quantities we are interested in (H_2 exhaust and the CDB distance). With an estimate for these two quantities in hand, the model at the current

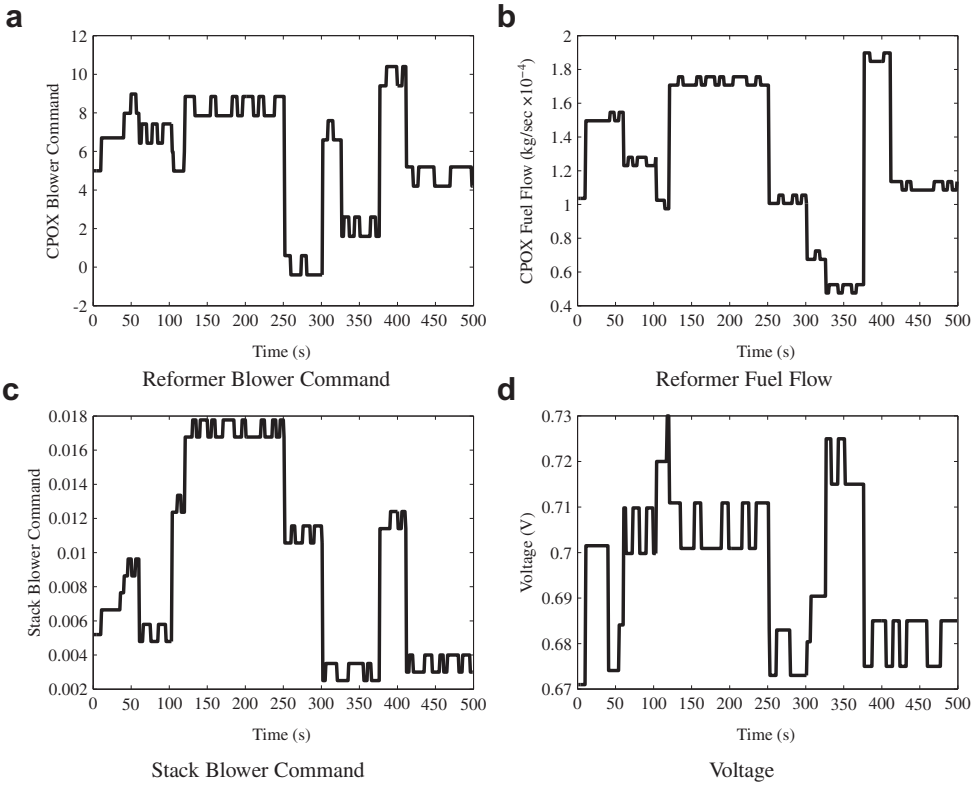

Fig. 5. Inputs used for identification simulation.

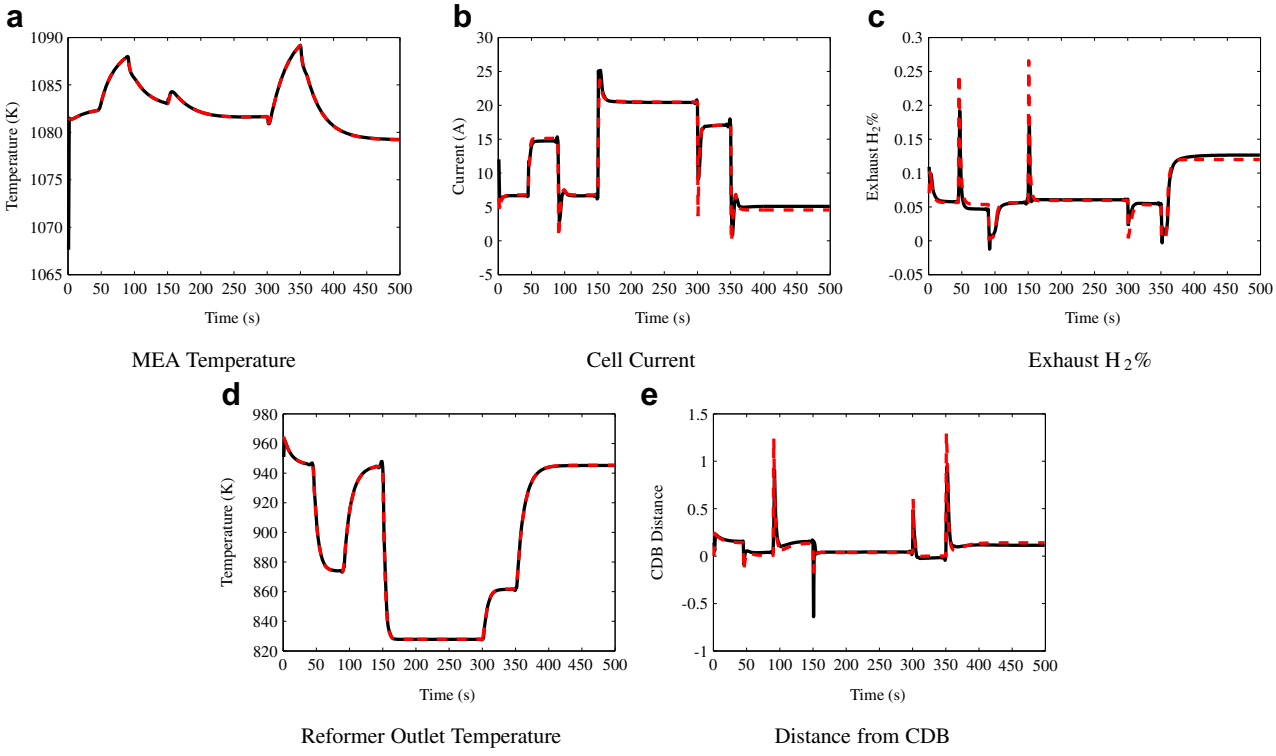

Fig. 6. System identification results, identified model is solid and black, nonlinear model is red and dashed. (For interpretation of the references to colour in this figure legend, the reader is referred to the web version of this article.)

time-step calculated and the desired current, the standard MPC optimization problem can be solved over a time window of N samples. The resulting quadratic cost optimization problem (Eq. (5)) gives the inputs to be applied at the next time-step.

Note that variables are as defined in Eq (2). A tracking implementation with a $N = 7$ step horizon is implemented with output weights only on the current, exhaust H_2% and the CDB distance. The demand current, target exhaust H_2% and target CDB distance are considered static over the horizon $(1 \ldots N)$ for the optimization

$$
\begin{aligned}
J = \underset{u}{\text{minimize}} \quad & x'_{k,N} P_f x_{k,N} + \sum_{i=0}^{N-1} x_{k,i}^T Q x_{k,i} + u_{k,i}^T R u_{k,i} + \left\| Q_Y \left(y_{k,i} - y_{\text{ref},i} \right) \right\|_2 \\
\text{subject to} \quad & y_{k,i}(1) \le 1200, i = 0, \ldots, N-1 \\
& y_{k,i}(3) \ge .025, i = 0, \ldots, N-1 \\
& 650 \le y_{k,i}(4) \le 1075, i = 0, \ldots, N-1 \\
& y_{k,i}(5) > 0, i = 0, \ldots, N-1
\end{aligned}
\tag{5}
$$

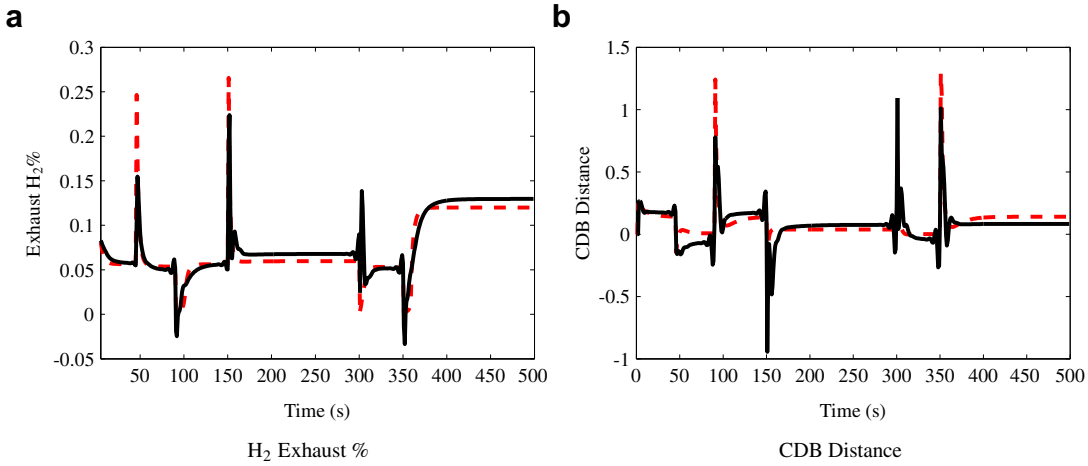

Fig. 7. LPV model results with Kalman filter. The LPV and Kalman estimate is black and solid, while the nonlinear model is dashed and red. (For interpretation of the references to colour in this figure legend, the reader is referred to the web version of this article.)

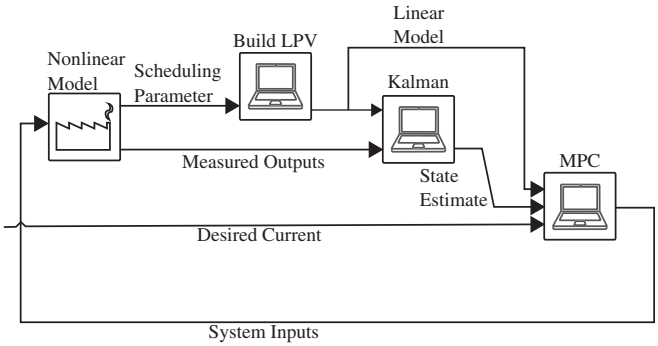

Fig. 8. MPC process flow.

Table 3
MPC weights.

Parameter	Value
Q_Y	$\begin{bmatrix} 0 & 0 & 0 & 0 & 0 \\ 0 & 10^5 & 0 & 0 & 0 \\ 0 & 0 & 1.0 & 0 & 0 \\ 0 & 0 & 0 & 0 & 0 \\ 0 & 0 & 0 & 0 & 1.0 \end{bmatrix}$
R	$\begin{bmatrix} 1 & 0 & 0 & 0 \\ 0 & 1 & 0 & 0 \\ 0 & 0 & 1 & 0 \\ 0 & 0 & 0 & 1 \end{bmatrix}$
Q	$\begin{bmatrix} 1 & 0 & 0 & 0 & 0 \\ 0 & 1 & 0 & 0 & 0 \\ 0 & 0 & 1 & 0 & 0 \\ 0 & 0 & 0 & 1 & 0 \\ 0 & 0 & 0 & 0 & 1 \end{bmatrix}$

problem in Eq. (5). They are also updated at every time step after applying the calculated inputs. The weighting for the current is five orders of magnitude larger than that of the exhaust H_2% and CDB distance. This weighting has the effect of primarily ensuring the demand current is met. The smaller weights push the controller to keep the exhaust H_2% and CDB distance above their hard constraint minimums. This stabilization is to account for modeling error, forcing the controller to operate at some distance from the hard constraints. The state and input weights are both set to identity as the only requirement is to stay within hard constraints. In order to enforce stability, a terminal weight is added to the states. This weighting matrix P_f is chosen as a solution to a Riccati inequality [20]. All weights are summarized in Table 3.

5. Results

The controller was tested over a variety of output conditions. Results are shown for a current demand step both down and up of 1.0 A per second and 0.1 A per second in Fig. 9. In both cases the controller is able to closely meet the current demand, however the fast current step causes a much larger oscillation (Fig. 9(a)) than for the slow demand change (Fig. 9(d)). The output constraints are also violated for the large demand change, shown in Fig. 9(b) and (c). Violations occur for the exhaust H_2% constraint during the large current demand decrease. While violations of the CDB constraint occur for both current demand increases and decreases. However, the controller can stabilize the output current over the entire operating range (5–25 A). The controller is thus capable of load following while not violating any of the system constraints, for a limited rate of current change. The reason that the current trajectory rate change must be limited is that the MPC controller

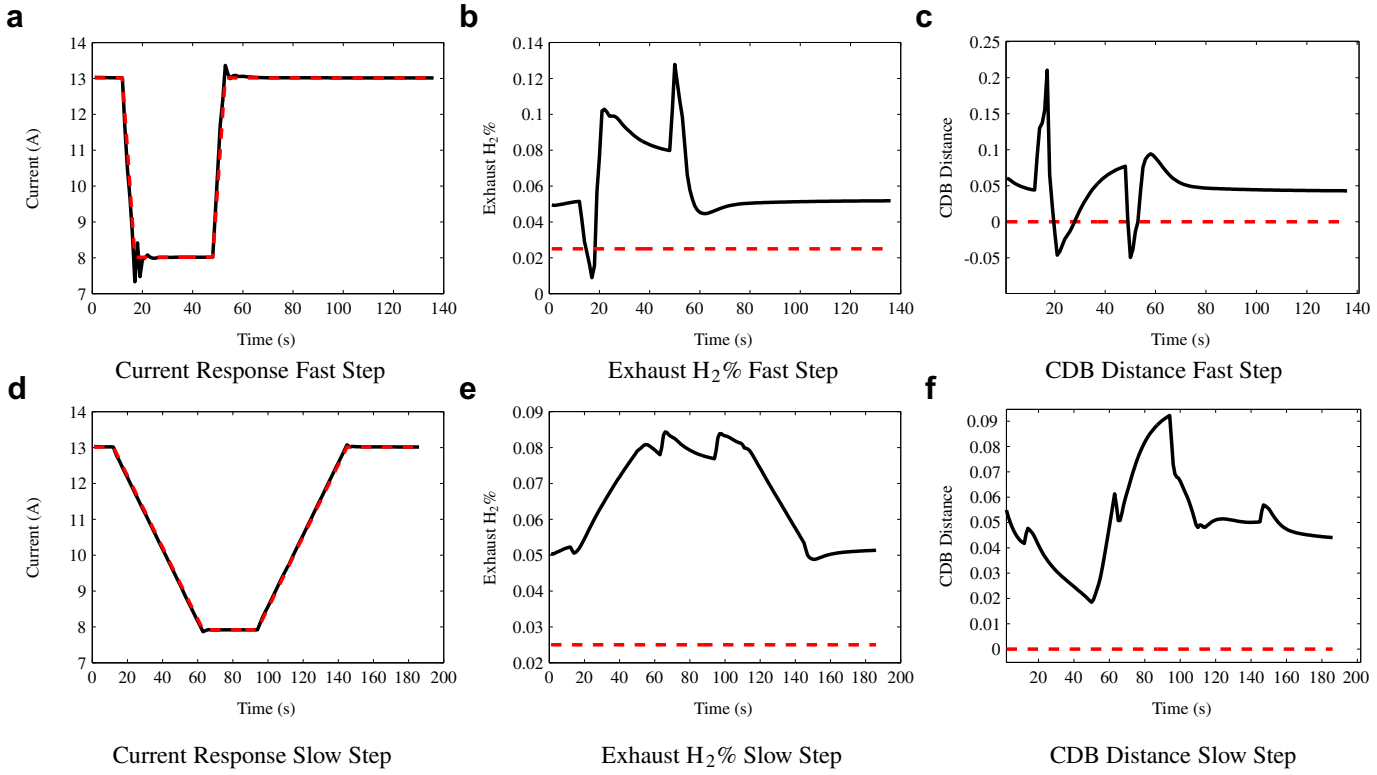

Fig. 9. Controller results for a fast and slow current demand change. The current demand curve is dashed and red, as are hard constraints. system response is solid and black. (For interpretation of the references to colour in this figure legend, the reader is referred to the web version of this article.)

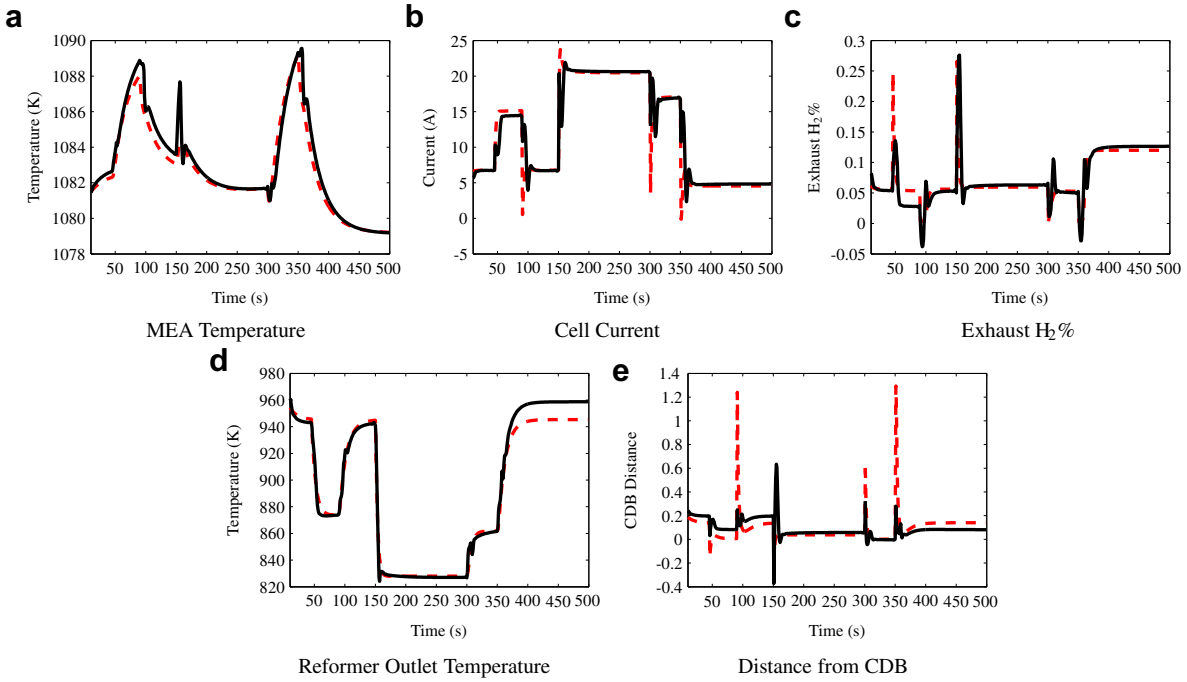

Fig. 10. $k = 7$ step predictor, identified model is solid and black, nonlinear model is red and dashed. (For interpretation of the references to colour in this figure legend, the reader is referred to the web version of this article.)

operates over a prediction horizon. The model used for the optimization is generated from the LPV model and fixed over this prediction horizon. A fixed linear model greatly decreases the complexity of the resulting optimization problem, but introduces modeling error. To visualize the model discrepencies faced by the controller, we utilize a k-step predictor where k is equal to the MPC horizon. The results of a $k = 7$ step predictor are shown in Fig. 10. The controller model faces large transient errors in H_2 exhaust concentration and CDB distance over the horizon, as shown in Fig. 10(c) and (e). These results are for the same input sequence as that used in Figs. 6 and 7.

The MPC controller thus has a discrepency between the predicted dynamics, which are used for the optimization, and the dynamics which are used for the optimization at each successive time step. If the current demanded is allowed to undergo large step changes, the dynamics at the next time-step may be different than predicted, and thus the calculated inputs will show a large error. The controller will eventually converge to a new model, but oscillation will occur around the new set-points. The magnitude and length of the oscillation is dependent on how far away the current MPC model is and thus how inaccurate the effects of the calculated outputs. Violation of hard constraints can occur during these changes as well for the same reasons. The MPC still calculates inputs that do not cause output violations, but the model it uses to do so is inaccurate over the horizon. In addition this mismatch is not equal at all operating points. For some regions, the LPV model is very close, thus allowing fast current changes, in other regions, the LPV model is inaccurate, requiring a limitation on the allowed magnitude of current change. The effect of this mismatch is prominently displayed in errors between the MPC predicted current (or the current demanded) and the actual system current which is measured.

Minimizing the MPC prediction horizon reduces the effect of this error, but increases the controller costs and can result in an infeasible problem. Implementing some form of LPV MPC should greatly reduce this problem, although with a cost of increasing the complexity of the controller. Alternatively, the rate of change for the scheduling variables can be limited. For the SOFC system, this requires limiting the allowed rate of current demand change. The controller has no difficulty avoiding constraints with a current demand change of 0.1 A. The use of a battery or capacitor will be required to limit the magnitude of the desired load change to such a value.

6. Conclusion

Current challenges in SOFC operation are often related to durability and carbon formation, this work has demonstrated a controller which can mitigate these design challenges. The controller is capable of staying within all desired operating temperatures as well as ensuring the reformer produces a fuel which is not prone to carbon formation, provided the magnitude of the load change is limited. The system identification algorithm requires only an existing first principles model which can produce input/output data over the operating range. Linear MPC is used, which is both fast and well established.

Acknowledgments

The authors would like to thank Dr. Neal Sullivan and Dr. Bob Kee for helpful discussions regarding fuel cell system operation and modeling.

References

[1] V.M. Janardhanan, V. Heuveline, O. Deutschmann, Journal of Power Sources 172 (2007) 296–307.
[2] E.D. Wachsman, K.T. Lee, Science 334 (2011) 935–939.
[3] S. Farhad, F. Hamdullahpur, Y. Yoo, International Journal of Hydrogen Energy 35 (2010) 3758–3768.

[4] K. Kattke, R. Braun, A. Colclasure, G. Goldin, Journal of Power Sources (2010).
[5] O. Deutschmann, R. Schwiedernoch, L. Maier, D. Chatterjee, Studies in Surface Science and Catalysis 136 (2001) 251–258.
[6] S. Gelfi, A. Stefanopoulou, J. Pukrushpan, in: Proceedings of the 2003 American Control Conference (2003), pp. 2049–2054.
[7] W.F. Stoecker, Design of Thermal Systems, International Student Edition, McGraw-Hill, 1971.
[8] M.J. Kupilik, T.L. Vincent, in: Control Applications (CCA), 2011 IEEE International Conference on, pp. 768–773.
[9] A.M. Colclasure, B.M. Sanandaji, T.L. Vincent, R.J. Kee, Journal of Power Sources 196 (2010) 196–207.
[10] D. Goodwin, Chemical Vapor Deposition XVI and EUROCVD 14 (2003) 2003–2008.
[11] M. Ansari, V. Mortazavi, Applied Thermal Engineering 26 (2006) 2401–2408.
[12] B.J. Spivey, T.F. Edgar, Journal of Process Control (2012) 1–19.
[13] G. Broers, B. Treijtel, Advanced Energy Conversion 5 (1965) 365–382.
[14] S. Farhad, F. Hamdullahpur, Journal of Power Sources 193 (2009) 632–638.
[15] J.-W. van Wingerden, M. Verhaegen, Automatica 45 (2009) 372–381.
[16] I. Houtzager, P. Gebraad, J.V. Wingerden, M. Verhaegen, Predictor-based Subspace Identification Toolbox Version 0.5 (2012).
[17] B.M. Sanandaji, T.L. Vincent, A.M. Colclasure, R.J. Kee, Journal of Power Sources 196 (2010) 208–217.
[18] H. Huo, X. Zhu, W. Hu, H. Tu, J. Li, J. Yang, Journal of Power Sources 185 (2008) 338–344.
[19] A.M. Murshed, B. Huang, K. Nandakumar, Computers & Chemical Engineering 34 (2010) 96–111.
[20] A. Bemporad, Robust Model Predictive Control: a Survey, Robustness in Identification and Control (1999).